Rossby soliton in the laboratory

S. V. Antipov, M. V. Nezlin, E. N. Snezhkin, and A. S. Trubnikov

Continuing our earlier experiments [JETP Lett. **33**, 351 (1981)], we have obtained in the laboratory and investigated, for the first time ever, Rossby solitary waves (solitons), which are the geophysical analog of two-dimensional drift solitons in a plasma. A Rossby soliton is observed in a thin layer of a rotating liquid and constitutes a long-lived nonspreading local vortex–anticyclone. It is in geostrophic equilibrium, i.e., the excess pressure at the center of the vortex is balanced by the centripetal Coriolis force that acts on the circular current of particles that rotate around the vertical axis of the vortex in a direction opposite to the global rotation of the liquid. The Rossby soliton drifts as a unit in a direction opposite to the motion of the liquid. Its lifetime is limited by the viscosity of the liquid: in pure water at a layer thickness $H_0 = 0.5$ cm it amounts to approximately 20 sec. During its lifetime, the Rossby soliton manages to drift over an approximate distance ten times its diameter and exhibits no noticeable spreading. This differs it in principle from a linear wave packet that spreads already over the mean free path equal to its own diameter. A strong asymmetry is observed in the conditions for the existence of vortices of opposite signs: there is no long-lived single cyclone (a well rotating in the direction of the liquid). The indicated structure of the Rossby soliton and its main parameters (dimension, drift velocity, natural rotation frequency, height and velocity profiles) agree on the whole with the theory of Petviashvili [JETP Lett. **32**, 619 (1980)] although some quantitative discrepancies are observed: the diameter of the soliton and its drift velocity are smaller by a factor 2 or 3 than in the theory, and these discrepancies are not connected with the viscosity of the medium. It is shown that the particles contained in the vortex drift together with the vortex, while the particles encountered in its path flow around the vortex. The paper presents a successful simulation of drift solitons in a plasma and can be regarded as supporting the qualitative aspect of that part of the Petviashvili theory according to which the giant red spot of Jupiter is a Rossby soliton. The quantitative aspect of the comparison of this theory with the observations of Jupiter was considered by Nezlin [JETP Lett. **34**, 77 (1981)].

PACS numbers: 47.30. + s, 47.35. + i

INTRODUCTION

We describe here the experiments initiated in Ref. 1, in which Rossby solitary waves (solitons) heretofore known only theoretically (see Ref. 2 as well as Refs. 3 and 4) were produced and investigated. Until recently, Rossby waves were predominantly the objects of the physics of media such as the atmosphere and the oceans of planets. In these media they play a fundamental role by determining the mechanism of large oceanic eddies[5] and exerting a substantial influence on the global circulation of the atmosphere.[6-8] At present Rossby waves are becoming of general physical interest: they probably have a direct bearing on such astrophysical phenomena as the famous eddy on Jupiter, known as the giant red spot,[2,4] and the heliomagnetic dynamo.[9,10] It has recently made clear[2,11,12] that they are physically similar to the drift waves so popular in plasma physics and in the problem of controlled thermonuclear fusion.[13,14] It seems useful therefore to publish our experimental paper precisely in a journal of general physical interest, all the more since we are dealing here not simply with Rossby waves, but with solitary waves or solitons, objects of fundamental interest for a number of branches of modern theoretical physics.[15,16] To make clearer the purpose of the present paper and the formulation of the problem, we precede the description of the experimental data by a brief summary of contemporary theoretical notions concerning Rossby waves, both linear (small amplitude) and solitary.

1. THEORETICAL NOTIONS CONCERNING ROSSBY WAVES AND SOLITONS

Rossby waves or planetary waves are produced in the atmosphere or in an ocean of a rotating planet, and feature low frequencies (ω) and large wavelengths (λ), namely $\omega \ll \Omega_0, \lambda \gg H_0$, where Ω_0 is the frequency of rotation of the planet and H_0 is the effective depth of its atmosphere. From the formally mathematical point of view, these waves were theoretically discovered on the basis of the Laplace tidal equations back at the end of the 19th century (see, e.g., the historical sketch in Ref. 17), but they started to attract great interest following a paper by the Swedish meteorologist Rossby,[18] who demonstrated their important role in geophysics (for contemporary reviews of Rossby waves see Refs. 19 and 20). A decisive role in the dynamics of Rossby waves is played by the Coriolis force. If the depth of the atmosphere (ocean) is not a function of the geographic coordinates, then Rossby waves result only from the spatial inhomogeneity (latitudinal gradient) of the Coriolis force, which causes vortical motion of the particles of the medium. The nature of these waves can be explained in the following manner. Consider a homogeneous atmosphere having a constant equivalent depth H_0 on a planet rotating with angular velocity Ω_0 (the planet rotates counterclockwise when observed from the endpoint of the vector Ω_0). According to the Kelvin-Helmholtz theorem concerning the conservation and freezing-in of a potential vortex, we have

$$\frac{d}{dt}\left(\frac{\text{rot } \mathbf{v} + 2\Omega_0}{H_0}\right)_z = 0, \tag{1}$$

where $\mathbf{v}$ is the flow velocity in the medium, and z is the local vertical coordinate that varies along the normal to the surface of the atmosphere at the point in question. Equation (1) was written for vector components along the local vertical, and accordingly $\Omega_{0z} = \Omega_0 \cos\alpha$, where α is the angle between the local z axis and the direction of the vector Ω_0, i.e., the complement of the

latitude angle. Let some perturbation take place in the atmosphere and some points of a certain parallel (for the sake of argument, in the northern hemisphere) to shift to the north, while other points are shifted to the south (Fig. 1, see also Ref. 19, where the explanation that follows is given). The displaced positions of the points considered are shown by the solid lines. Since the vertical projection Ω_{0z} of the vector Ω_0 increases in the northward direction, it follows from theorem (1) concerning the conservation of the total vortex (curl v $+ 2\Omega_0)_z$, the quantity (curl v)$_z$ should decrease in the case of northward displacements and increase for southward displacements. Therefore the deviation of the points to the north causes a compensating vortex opposite to Ω_{0z}, and the deviation of the points to the south creates a vortex directed along Ω_{0z}, as shown by the arrows in Fig. 1a. As a result, the produced perturbation will shift to the position shown by the dashed curves, i.e., it will be displaced (drift) to the west, opposite to the global rotation of the planet. This is in fact the Rossby wave, which always drifts westward. The Rossby wave is thus the result of the spatial inhomogeneity of the Coriolis force. It follows directly from (1) that the Rossby wave can also be due to a gradient of the depth of the atmosphere: if, e.g., the depth of the atmosphere increases in the southern direction, then the drift velocity of the Rossby wave increases, and when the gradient of the depth of the atmosphere has the opposite sign the wave velocity decreases.

The dispersion equation for the Rossby waves is given by[19, 20]

$$\omega = \frac{\beta k_x}{k_x{}^2 + k_y{}^2 + 1/r_R{}^2},$$ (2)

where ω is the angular frequency of the wave, k_x and k_y are wave numbers corresponding to oscillations along the parallel and the meridian, respectively, $r_R = (gH_0)^{1/2} f_0$ is the so called Rossby radius,

$$\beta = \frac{1}{r_R{}^2} \frac{\partial}{\partial y}(f_0 r_R{}^2) = \frac{1}{R r_R{}^2} \frac{\partial}{\partial \alpha}\left(\frac{gH_0}{f_0}\right),$$ (3)

$f_0 = 2\Omega_0 \cos \alpha$ is the Coriolis parameter, and R is the radius of the planet.
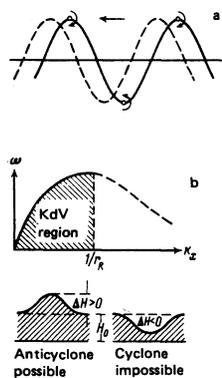

FIG. 1. Illustrating the mechanism of Rossby waves and solitions. The round arrows in the upper figure (a) denote cancelling vortices, and the horizontal arrow shows the direction of propagation of the wave (to the west). The system rotates from west to east; b) schematic form of the dispersion function $\omega(k_x)$.

Equation (2) was written for a so-called barotropic medium, whose density does not change in the vertical direction. This is precisely the case realized in the experiments considered below. The function $\omega(k_x)$ is shown schematically in Fig. 1. What is important in principle is that on the rising section $(k_x \lesssim 1/r_R)$ it corresponds to a situation in which the nonlinear wave is described by an equation of the Korteweg–de Vries (KdV) type, the very equation that yields soliton solutions also for other waves with dispersion of the same type (2), namely ion-sound waves in a plasma and gravitational waves in "shallow water" with depth less than the wavelength.[21, 22] Solitons should therefore be expected also in the case of Rossby waves, and were indeed deduced in a theoretical paper.[2] Just as other solitons describable by a dispersion function of the type (2), the Rossby soliton should have the following general properties: first, it must be only a hill-type wave and cannot be a well (see Fig. 1); second, its characteristic dimension (diameter), which decreases with increasing height, should be determined by a scale corresponding to the maximum of the dispersion curve (2) (in our case by the Rossby radius r_R); third, the soliton drift velocity relative to the medium should be somewhat larger (more the larger the soliton amplitude) than the maximum velocity of the linear waves (in our case the linear Rossby waves). An additional property of the Rossby soliton is that it is an isolated geostrophic equilibrium vortex rotating around its own vertical axis in a direction opposite to the global rotation of the system. In other words, the Rossby soliton is an anticyclone (see Fig. 1), in which the hydrostatic pressure in excess of the pressure of the surrounding medium is balanced by the Coriolis force acting on the circular current of the particles around the vortex axis. The Rossby-soliton height proper angular velocity have typical Gaussian profiles; its diameter $2a$ is defined as the width at mid-amplitude, and the characteristic frequency of its proper rotation ω_r is defined as the frequency of the revolution at the distance a from the center of the soliton. According to the foregoing, the Rossby soliton has in the theory of Ref. 2 the following parameters: its diameter is

$$2a \approx 3.5 r_R h^{-\frac{1}{4}},$$ (4)

where $h = \Delta H/H_0$ is the relative amplitude of the soliton and ΔH is the rise of the atmosphere; the soliton drift velocity in a direction opposite to the rotation of the system (i.e., to the west) is

$$V_x \gtrsim \left(\frac{\omega}{k_x}\right)_{\max} = \beta r_R{}^2 = \frac{\partial}{\partial y}(f_0 r_R{}^2),$$ (5)

where $(\omega/k_x)_{\max}$ is the maximum phase velocity of the linear Rossby waves, defined by relations (2) and (3); the characteristic soliton rotation frequency is

$$\omega_r/f_0 \approx \frac{1}{3} h^2.$$ (6)

When the soliton moves relative to the medium, its shape (height profile) is preserved: the dispersion spreading which is a characteristic of a linear packet is offset by the nonlinearity (the viscosity of the medium is not taken into account in the theory).

It must be borne in mind that the theory is valid only if the ratio a/R of the soliton radius to the curvature radius of the system is a small parameter. The requirement that the ratio a/R be small is of fundamental character and is connected by the fact that at sufficiently a/R the soliton is destroyed as a result of the appreciable difference between the drift velocities of its different parts. Let us explain this circumstance, which was pointed out by V. V. Yan'kov. It is easily seen from (5) that the difference between the drift velocities of diametrically opposite particles of the soliton (in the direction from the north to the south) is

$$\Delta V_x = \frac{\partial V_x}{\partial \alpha}\frac{2a}{R} = \frac{2(1+\sin^2\alpha)}{\cos^2\alpha}\frac{f_0 r_R^2 a}{R^2}. \tag{7}$$

To keep the soliton from falling apart, its characteristic velocity of rotation around its own axis, v_r, must exceed ΔV_x by at least π times, i.e., the condition

$$v_r \gtrsim \pi \Delta V_x \tag{8}$$

must be satisfied. The rotation velocity $v_r = \omega_r a$ is defined by relation (6), so that the condition (8) takes the form

$$\frac{2a}{R} \lesssim \sqrt{2}\left(\frac{r_R}{R}\right)^{1/2} \tag{9}$$

or

$$\frac{2a}{r_R} < \sqrt{2}\left(\frac{R}{r_R}\right)^{1/2}. \tag{10}$$

In the case of the parabolic model used in our experiments, the condition (8) likewise takes the form (10).

The described Rossby waves are similar to drift waves in a plasma, and the Rossby soliton is analogous to the two-dimensional drift-wave soliton deduced theoretically in Ref. 12. The point is that the trajectories of the (neutral) particles of the atmosphere or the ocean, which transport the Rossby waves, are twisted by the Coriolis force in approximately the same manner as the plasma charged-particle trajectories are twisted by the Lorentz force. The quantity analogous to the Coriolis parameter $f_0 = 2\Omega_0 \cos\alpha$ in the Rossby wave is in the plasma case the Larmor frequency ω_H of the ions. Just as the Rossby-wave frequencies are lower than f_0, the driftwave frequencies are lower than ω_H. The dispersion of the drift waves is determined essentially by the Larmor radius of the ions at the electron temperature, $r_i = (T_e/M)^{1/2}/\omega_H$, which is the plasma analog of the Rossby radius. The dispersion equation of the drift waves is similar to (2). Just as the Rossby waves result from a spatial gradient of the Coriolis force and of the hydrostatic pressure, the drift waves result from the presence of a plasma-pressure gradient. Both types of wave propagate around the longitudinal axis of the system perpendicular to the indicated gradients. The maximum wave velocity in this direction is in the case of the Rossby wave $(\omega/k_x)_{max} = f_0 r_R^2/a_0$, and in the case of the drift wave $\omega_H r_i^2/a_0$, where a_0 is the characteristic dimension of the gradients of the quantities T_e and gH_0 ($a_0 = R/\sin\alpha$ in the case of an atmosphere or an ocean). The nature of the drift waves can be explained by the same Fig. 1, by considering the Lorentz force in place of the Coriolis force, the ion Larmor frequency ω_H in place of the Coriolis parameter, and the plas-

ma pressure nT in place of the hydrostatic pressure gH_0 (n is the density and T is the temperature). The analogy between the two wave types is thus sufficiently complete.

According to the theory of Ref. 2, the vortex observed as the giant red spot on Jupiter is a Rossby soliton (see also Ref. 4). This view is in qualitative agreement with the observations, although there are considerable quantitative discrepancies between the theory and the observations on Jupiter. A possible way of eliminating these discrepancies is to take into account the vertical wave motion in the spot (soliton). That this procedure can result in good quantitative agreement between the theory and the observation data is demonstrated in Ref. 23.

2. FORMULATION OF PROBLEM, EXPERIMENTAL SETUP AND TECHNIQUE

We have thus shown in the preceding section that isolated Rossby waves (solitons) are a probable natural phenomenon and simulate adequately drift solitons in a plasma. An attempt was therefore undertaken to produce and investigate them in the laboratory—this was the main purpose of the present study. No solitary Rossby waves were observed in the laboratory before. In all the preceding experiments with Rossby waves[24-27] they studied either the properties possessed by linear waves, or else the nonlinearity (if it appeared at all) played no fundamental role in the sense that it never compensated for the dispersion spreading. Therefore the Rossby-wave packets excited in some experiments spread very rapidly because of the uncompensated dispersion (see, e.g., Ref. 25, p. 89 of the translation and Fig. 2.16).

In the experiments described below (and started in Ref. 1) solitary vortices were produced for the first
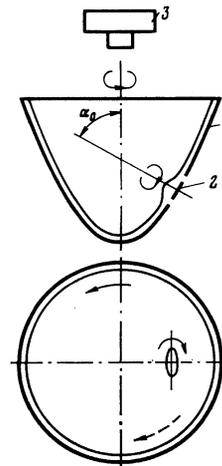
FIG. 2. Diagram of experimental setup: 1) vessel having a bottom with a parabolic profile; 2) rotating "pumping disk"; 3) motion-picture or still camera. The paraboloid rotates counterclockwise around a vertical axis. The dashed arrow on the view from the top shows the direction of the Rossby-solition drift. The soliton lags the global motion of the liquid. The normal to the liquid surface at the working point makes an angle α_0 with the vessel rotation axis.

time, and it was verified that they are Rossby solitons. The method whereby the investigated vortices were identified as Rossby solitons consisted of measuring all the parameters of the vortices and comparing them with the theoretical relations (4)–(6), and (10). In the measurements of the vortex drift velocities it was necessary to take into account certain important circumstances not considered above. The point is that Rossby waves are usually considered in the atmosphere of a planet (or in the ocean), and it is stated that they are due to a gradient of the Coriolis force. On the other hand, to imitate in the laboratory effects connected with a gradient of a Coriolis force, the experiments were performed with a liquid in a straight cylinder with sloping bottom. In such a geometry, the effect due to the gradient of $1/H_0$, as shown above (see also Refs. 24–27) turns out to be equivalent to the effect of changing the Coriolis parameter f_0 under natural conditions. At the same time, the dynamics of the Rossby waves is in fact determined by the spatial gradient of the quantity $g^* H_0/f_0$, where g^* is the effective acceleration of the resultant of the gravity and centrifugal forces. (In the case of a planet $g^* \approx g$, but in the experimental setup considered below $g^* = g/\cos\alpha$.) Thus, according to (2), (3), and (5) the maximum velocity of the Rossby waves (which turn out to differ little from the Rossby-soliton velocity) is proportional to the spatial derivative of the product of three quantities, each of which is a function of the meridional coordinate y:

$$V_x \gtrless \left(\frac{\omega}{k_x}\right)_{max} = \frac{g^* H_0}{f_0^2}\frac{\partial f_0}{\partial y} - \frac{H_0}{f_0}\frac{\partial g^*}{\partial y} - \frac{g^*}{f_0}\frac{\partial H_0}{\partial y}. \quad (11)$$

In expanded form, as applied to the parabolic model considered below, where $g^* = g/\cos\alpha$ and R is the curvature radius of the meridian, the Rossby-wave velocity relative to a rotating liquid (or the soliton drift velocity, which is somewhat higher) is determined by

$$V_x \gtrless \left(\frac{\omega}{k_x}\right)_{max} = -\frac{1}{R\cos^2\alpha}\left(\frac{gH_0}{f_0}\sin\alpha + \frac{gH_0}{f_0}\sin\alpha + \frac{g}{f_0}\cos\alpha\frac{\partial H_0}{\partial\alpha}\right). \quad (12)$$

Whereas in the laboratory one observes usually effects connected only with the third term in the right-hand side of (12) (see, e.g., Refs. 24–27), we must also bear in mind and investigate the relation (12) in the general case.

The direct object of the investigation was chosen to be "shallow water" of approximately constant depth in a vessel having a bottom with parabolic profile and rotating about a vertical symmetry axis (Fig. 2). This choice of the vessel shape was dictated by the fact that only a paraboloid makes it possible (at a certain rotary speed) to have a constant liquid depth independent of the coordinates and, in particular, to study the drift of Rossby vortices at constant H_0. No experiments with Rossby waves were heretofore performed in such a geometry. The geometry of the paraboloid was the following. Its maximum inside diameter was 28 cm. At a rotary frequency of the vessel $\Omega_0/2\pi = 1.7$ Hz the water formed a uniform layer of depth $H_0 = 5$ mm on the bottom of the vessel.[1] The shape of the water surface in a meridional section (i.e., in an intersection of a vertical plane passing through the rotation axis) corresponded to

the equation

$$gz = \Omega_0^2 r^2/2 \quad \text{or} \quad z = 6 \cdot 10^{-2} r^2, \quad (13)$$

where z and r are the vertical and horizontal coordinates of the point on the liquid surface. In this model situation the hydrostatic pressure of the liquid is determined by the resultant of the gravity force and the centrifugal force due to the global rotation of the liquid. The acceleration of the resultant is

$$g^* = g/\cos\alpha. \quad (14)$$

In this geometry the Rossby radius is given by

$$r_R^2 = gH_0/f_0^2\cos\alpha. \quad (15)$$

By choosing the proper rotary speed of the paraboloid it was possible to produce a liquid-depth gradient directed either towards the periphery of the vessel (at $\omega_0/2\pi > 1.7$ Hz) or towards the center of the vessel (at $\omega_0/2\pi < 1.7$ Hz). The influence of the change of the rotary frequency of the vessel on the Rossby velocity is described by a relation that takes the simplest form for that parallel on the paraboloid which is located at a distance $r_0 = R_0\sqrt{2}$ from the rotation axis, where R_0 is the radius of the vertical cylinder bounding the transverse dimension of the paraboloid. In our experiments $r_0 = 10$ cm and the indicated relation takes the form

$$V_x \gtrless \left(\frac{\omega}{k_x}\right)_{max} \quad (16)$$
$$= H_0\Omega_0\sin\alpha\left(1 + \frac{R/H_0}{1+\Omega_0^4 R_0^2/2g^2}\frac{\Delta\Omega}{\Omega}\right)$$

or

$$V_x \gtrless \left(\frac{\omega}{k_x}\right)_{max} = H_0\Omega_0\sin\alpha\left(1 \pm \frac{R}{L_H}\frac{\text{ctg}\,\alpha}{2}\right), \quad (16')$$

where α is the angle between the horizontal and the tangent to the parabola (13), $\tan\alpha = \Omega_0^2 r/g$; $\Delta\Omega$ is the deviation of the paraboloid rotary frequency from the frequency Ω_0 corresponding to a uniform liquid layer (grad $H_0 = 0$), $\Delta\Omega \ll \Omega_0$; y is the meridional coordinate ("latitude") on the surface of the paraboloid, $dy = Rd\alpha$;

$$L_H = H_0 \left/ \frac{\partial H_0}{\partial y}\right.$$

is the characteristic dimension of the gradient of the depth of the liquid. In the experiment, the coordinates of the working point where the vortex was produced were $r = 10$ cm and $z = 6$ cm, the radius of the curvature of the parabola at this point was $R = 32$ cm, $\cos\alpha = 0,6$; $r_R = 2.1$ cm at $H_0 = 0.5$ cm.

To excite a solitary Rossby vortex, a thin metallic disk of 3 cm diameter was placed at the chosen working point near the bottom of the liquid. The disk was rotated around the normal to the parabola at the working point and gradually produced local rotation in the liquid above it. We note immediately that the disk diameter was varied in the experiments; the value cited here corresponded to the optimal excitation of the long-lived vortices (this will be discussed in greater detail below). The experiments have shown that when the disk was rotated in the "necessary" direction, i.e., against the rotation of the vessel (see Fig. 2), there is separated from the "pumping disk" a geostrophically equilibrium anticyclonic vortex—a liquid prominence rotating around

its own vertical axis, having a height ΔH (which is the amplitude of the investigated vortex) determined by the adjustable frequency and duration of the disk rotation. A typical vortex amplitude was $\Delta H = H_0/2$ ($h = 0,5$). A Coriolis force directed towards the center of the vortex prevented this anticyclone from being spread by the gravitational force and by the centrifugal force of the global rotation of the liquid [see Eq. (17) below]. (The centrifugal force connected with the rotation of the vortex about its own axis can be neglected.)

After the formation of the local vortex, the pumping disk was stopped and the surface of the liquid was photographed either with a fixed motion-picture camera located over the vessel, or with a photographic camera rotating with the vessel. The bottom of the vessel was covered with white paint that reflected white light diffusely, and the liquid was observed in the transmitted light reflected from the white bottom. The working liquid in most experiments was a green solution of nickel sulfate. The photography was through a red light filter, so that the local rise of the green liquid appeared as a dark spot on the positive. The spatial and energy characteristics of the vortices (amplitude, height profile, transverse dimensions) were measured by photometry of the negatives.

The velocity field in the vortex was determined with a camera that rotated together with the paraboloid. To visualize the velocity field we used white paper circles of 1 mm diameter floating on the surface of the liquid. By measuring the length of the circle trajectory at a given (controlled) photographic exposure, we were able to determine the current velocities in the vortex and estimate independently the rate of the vortex drift relative to the liquid. (The drift velocity was measured more accurately by taking motion pictures of the vortex motion.) These measurements determined also an important nonlinearity parameter, namely the ratio of the characteristic vortex angular velocity to its drift velocity. In accordance with relations (8) and (18) below, this parameter determines the stability of the vortex and its interaction with the particles of the liquid. To investigate the character of this interaction, and specifically to determine whether the vortex entrains external liquid particles as it drifts, special experiments were performed. In these experiments, catapults were used to hurl test particles (white paper circles in one set of measurements and droplets of potassium permanganate solution in another) either from the top on the region of the vortex or ahead of the vortex in its drift direction. The two types of test particle differed in that the paper circles could float only over the surface of the liquid, whereas the droplets of potassium permanganate could also sink into it. The working liquid in these experiments was pure water and the viscosity of the liquid was considerably (by an approximate factor of 3) lower than in the experiments with the solution of nickel sulfate. The experiments provided therefore also an answer to the fundamental question of the influence of the viscosity of the medium (not accounted for in the considered theory[2]) on the properties of Rossby solitons and on its principal parameters such as the size, drift velocity, and lifetime (free path).

3. EXPERIMENTAL DATA AND COMPARISON WITH THE THEORY

The experiments have shown that if the amplitude of the perturbation over the rotating pumping disk is not too small, then immediately after the disk rotation is stopped (more accurately, even before it is stopped), an anticyclonic vortex is separated from the disk. This vortex rotates around its own vertical axis in a direction opposite to the vessel rotation and the water level over the disk returns rapidly to the level of the surrounding liquid. The vortex produced in this manner lags the globally rotating liquid, i.e., it moves (drifts) over the surface of the paraboloid in a direction opposite to the rotation of the vessel. The lag of the vortex relative to the pumping disk at $H_0 = 0.5$ cm = const is approximately 8° of arc for each revolution of the paraboloid. The foregoing is illustrated in Figs. 3–5, which
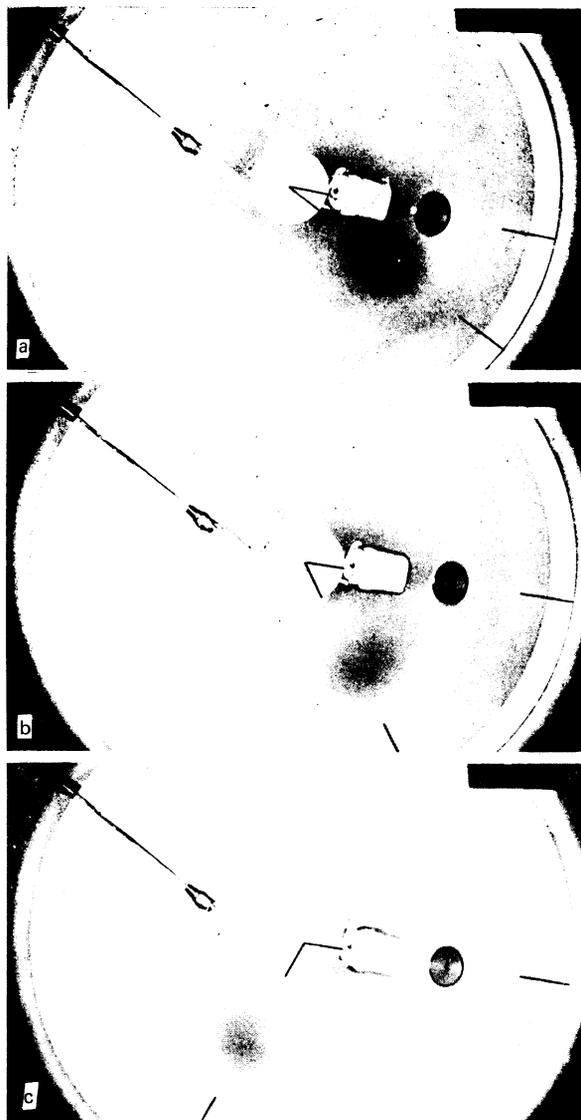

FIG. 3. Photographs of the surface of the rotating liquid with excited Rossby soliton. For clarity, the angular displacement of the vortex relative to the pumping disk is marked by short lines at the center of the vessel and on the periphery. Quantitative data on the vortex drift velocity are shown in Figs. 4–6.

show motion-picture photographs of the drift of the vortex (taken with an immobile motion-picture camera) and the rate at which it lags the liquid. In particular, Figs. 4 (curve drawn through light circles) and 5 shows the rate of the vortex drift in the experimental run in which the working liquid was pure water (the viscosity of the medium was decreased by an approximate factor of 3). It is seen that the decrease of the viscosity of the medium increases considerably the lifetime of the vortex, but does not change the drift velocity. It is also seen that the characteristic dimension (diameter) of the vortex remains approximately constant during the observation time and amount at $H_0 = 0.5$ to approximately 5 cm, i.e., 2.5 Rossby radii, independently of the viscosity of the medium. [Figure 5 calls for an explanation. The point is that the droplet of potassium permanganate is injected into the vortex (from the top) in the form of a thin strip in its diametral plane. As a result, the angular velocity of the particles in the vortex is larger towards the center (see Fig. 10 below), the strip of potassium permanganate is twisted by the vortex into a double helix: the outer sections of the strip are twisted with a smaller angular velocity than the inner ones.]

When the frequency of the paraboloid rotation changes, i.e., under conditions when the depth of the liquid has a gradient along the meridian, all the phenomena described here remain qualitatively the same, but the vortex drift velocity (its lag relative to the vessel rotation) changes: it increases if the depth of the liquid increases towards the periphery of the paraboloid, and decreases when the depth gradient is of opposite sign. In particular, at a definite vessel rotation frequency, the drifts due to the gradients of the Coriolis force, of the effective acceleration g^*, and of the depth of the liquid cancel each other completely, and the vortex is stopped (relative to the liquid). In other words, there exists a critical vessel angular velocity starting with which the drifting vortex is observable. This is illustrated in Fig. 6. Attention is called to the fact that when the angular velocity of the paraboloid is changed by only 2.5–3% the vortex drift velocity changes quite significantly, increasing by approximately a factor of 1.5 or decreasing to zero. Special attention was paid therefore to maintenance of a constant (unaccelerated) rotation of the vessel. The rotation period was continuously measured with a Ch3-34 quartz stopwatch and was main-
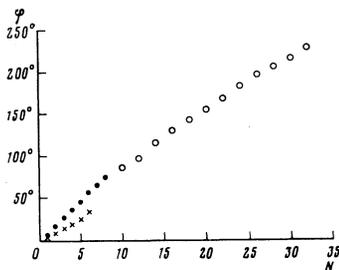

FIG. 5. Drift of anticyclone vortex (clockwise, against the vessel rotation) in an experiment with pure water as the working liquid. The time interval between the frames is approximately 8 sec. The lifetime of the vortex is approximately 20 sec; 1) pumping disk, 2) catapult.

tained constant with accuracy not worse than 0.5%. All the regularities of the vortex drift agree well with the theoretical relations (16). The numerically measured drift velocities turned out to be half the value of $(\omega/k_x)_{max}$ given by (16). This means that the investigated vortex drifts at a rate approximately one-third the theoretically prescribed value.[2]

FIG. 4. Dependence of the angular displacement of the vortex (φ) relative to the pumping disk on the time measured in the number N of the vessel revolution; × ●) working liquid–nickel sulfate, $H_0 = 3$ mm (×) and $H_0 = 5$ mm (●); ○) working liquid pure water, $H_0 = 5$ mm; in this case the vortex lifetime is approximately 20 sec.
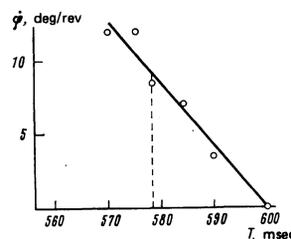

FIG. 6. Dependence of the velocity of the angular displacement of the vortex on the paraboloid revolution period, $H_0 = 0.5$ cm. When the revolution period is decreased in comparison with the "normal" (579 msec, shown dashed) a liquid-depth gradient is produced, directed towards the periphery of the vessel; when the revolution period is increased (at $T > 579$ mesc), a liquid-depth gradient directed towards the center of the vessel is produced. H_0 is constant at $T = 579$ msec.

The characteristic vortex lifetime τ, after which its height becomes barely distinguishable, is determined by the viscosity of the liquid. Thus, in experiments with nickel sulfate the value of τ was approximately 5 sec (8–9 revolutions of the paraboloid). This time is hundreds of times longer than would take for gravitational equalization of the perturbation in the absence of the (centripetal) Coriolis force. In the experiments with pure water (with the vortex region colored by droplets of potassium permanganate) the value of τ increased, according to Figs. 4 and 5, by 3–4 times and reached 20 sec at $H_0 = 0.5$ cm, corresponding approximately to the estimate $\tau \approx H_0^2/\nu$, where ν is the kinematic viscosity of the liquid. During this lifetime the observable anticyclone vortex manages to drift over a distance exceeding quite appreciably its diameter. This is seen already from Fig. 3 (the working liquid is the relatively viscous solution of nickel sulfate), but particularly from Figs. 4 and 5, where the working liquid is pure water, i.e., a medium having one-third the viscosity. In the latter case the vortex drifts over a distance equal to ten of its diameters and without any noticeable change in shape. This property (non-spreading) of the observed vortices distinguishes them in principle from the classical (linear) wave packet, which is known to spread rapidly as a result of dispersion before it manages to negotiate a distance equal to its own size. (An example of the dispersion spreading of a wave packet, as applied to Rossby waves, was already given above; see also Ref. 25, p. 89 of the Russian translation and Fig. 2.16.)

Thus, the observed vortex behaves as an isolated nonlinear wave—a soliton. And since its dimensions and drift velocity agree within a factor 2–3 with all the predictions of the theory [see relations (4), (5), (15), and (16)], the vortex can be identified as a Rossby soliton.

One of the most radical results, which is quite clearly revealed in the described experiment, is due to the observed patent asymmetry under conditions when vortices of opposite sign, anticyclones and cyclones, are present. All the experimental data on the long-lived single vortices reported in this paper pertain to anticyclones. There are simply no long-lived single cyclones: they could not be produced by any vortex-excitation method. This fundamental question calls for an explanation. It might seem that by reversing the direction of the rotation of the pumping disk it is possible to produce a cyclone vortex just as successfully as the anticyclones described above. Experiment shows that during the time that the disk is rotated in the "incorrect" direction, which coincides with the direction of rotation of the vessel, a perturbation of the cyclone type does exist over the disk and in its neighborhood, with a local decrease of the height of the liquid (the Coriolis force is directed in this case away from the center of the pump disk and produces a well). After the disk is stopped, however, the produced well is rapidly filled by the liquid and does not leave a non-spreading cyclone. Moreover, even in this case, instead of the expected cyclone there appears an anticyclone coming from places adjacent to the region of the cyclonic excitation. This
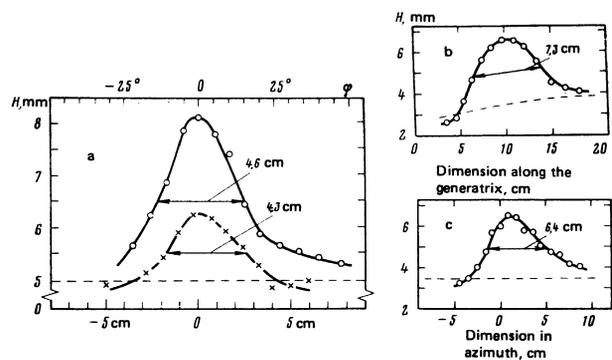

FIG. 7. a) Azimuthal profiles of the height of an anticyclone ($H = H_0 + \Delta H$) at different anticyclone amplitudes. Dashed—unperturbed height of the liquid: $H_0 = 0.5$ cm. The abscissas are the distances from the center of the vortex. The arrows show the width of the profile at half-amplitude level—the soliton diameter; b, c) soliton profiles in two directions at H_0 = 0.3 cm and $h \approx 1$. It is useful to compare this figure with Fig. 10.

asymmetry is evidence of the fundamental nonlinearity of the observed vortices, and by the same token, is most convincing evidence favoring the theory[2] considered in Sec. 1.

Figure 7a shows the spatial profiles of the height of the liquid in the vortex at different vortex amplitudes. The profiles were obtained by photometry, which shows that they have the bell-shaped soliton form. In the amplitude range $h = 0.25$–0.65 the transverse dimension of the vortex is practically independent of its amplitude and turns out to equal approximately 4.5–5 cm $\approx 2.5 r_R$. The profiles of Fig. 7a are drawn along the longitudinal coordinate—in the direction of the vortex motion. It is seen from Figs. 7b and 7c, which show also the transverse profile, that the vortex has approximately axial symmetry about its own vertical axis. Figures 7b and 7c correspond to an amplitude $h \approx 1$, which is close to the maximum possible: at a larger amplitude (which can be reached only at high pump-disk rotary speed), foam is produced. On the other hand, at $h < 0.2$, the photometry becomes inaccurate. In addition, at $h < 0.2$ the soliton size expected in accordance with the relation (4) becomes so large that the conditions (9) and (10) are not satisfied and the theory no longer applies to our experiment. Thus, the indicated photometry range covers practically the entire range of parameters within which experiment can be compared with theory.

It is interesting to compare the data on the real dimensions of the observed vortices with the theoretical relation (4). The vortex diameter turns out in experiment to be smaller than would follow from (4), by an approximate factor of 3 at amplitudes of the order of $h \approx 0.25$ and by approximately one-half at $h \approx 0.6$. Only in the case of the largest measured amplitude, $h \approx 1$ (the conditions of Fig. 7b and 7c, $H_0 = 0.3$ cm) is the size of the vortex formally practically equal to the theoretical value, if it is assumed that Eq. (4) can be used even at $h = 1$... (it is assumed in this theory that $h < 1$). The independence of the sizes of the observed vortices of their amplitude, expressed by the series shown in Fig.

7a, seems at first glance to contradict relation (4). Account must be taken here, however, of the following two circumstances. First, according to condition (10) the soliton diameter must not exceed 10 cm. In our experiments this limitation sets in earlier and it turns out that $2a \lesssim 5-7$ cm. Second, with the increasing soliton amplitude the depth $(H_0 + \Delta H)$ of the liquid increases, i.e., the Rossby radius r_R increases, and this also slows down the decrease of the soliton. In our opinion, these circumstances explain the experimental irregularities considered here.

The isolated vortices described so far are produced under conditions such that the pumping disk rotates for a relatively long time and is stopped immediately after one anticyclone is detached from it. If, however, the pumping disk is not stopped immediately after the formation of one vortex, but is rotated somewhat longer, experiment shows that the disk generates a whole anticyclonic "train" in which further interesting transformations take place. Figure 8 shows examples of such transformations. It is seen that structures made up of coupled vortices are produced. Thus, in case *a* a cyclone-anticyclone "pair" is produced (the cyclone is lighter than the anticyclone), and in case *b* the vortex system consists of two anticyclones and one cyclone between them (the latter is seen as a lighter spot against the background of the surrounding liquid). These structures exist for sufficiently long time, approximately as

long as single anticyclones. The fact that these structures contain also cyclones does not contradict the earlier conclusion that there are no single cyclones. Cyclones contained in vortex structures are secondary formations, "untwisted" anticyclones; they rotate much more slowly (this will be discussed in greater detail below).

Figure 8 leads to the following important conclusion: The observed vortices into which the perturbed zone breaks up turn out to be much smaller than the perturbed zone, which in turn is considerably larger than the pumping-disk diameter. This means that the vortex dimensions are not "tied" to the size of the pumping disk, and also that to produce a sufficiently extended perturbation zone there is no need for a disk more than 3 cm in diameter. At the same time, experiments have
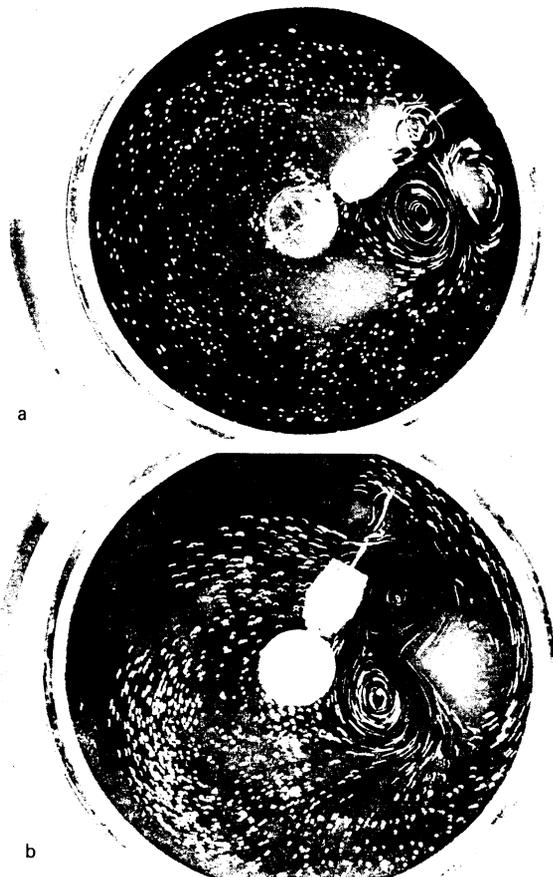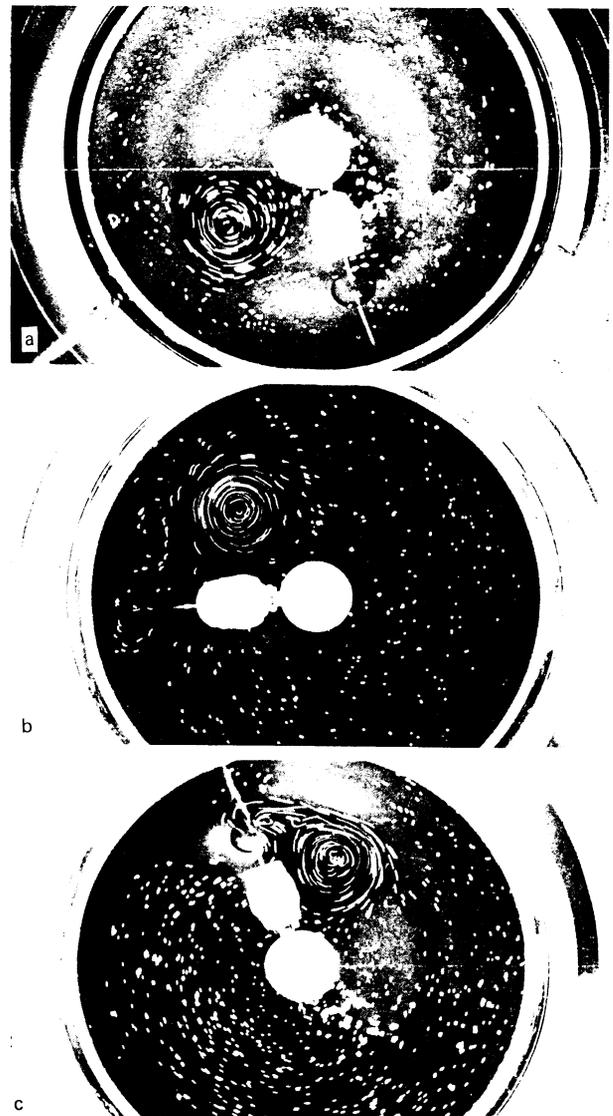

FIG. 9. Examples of anticyclone vortices visualized with the aid of white particles floating on the liquid surface, and also by contrast. The frames were taken 2–3 sec after stopping the pumping disk. Exposure of the camera (which rotated with the vessel): a) 1/4 sec, b) 1/2 sec, c) 1/4 sec.

FIG. 8. Examples of coupled cyclone-anticyclone structures.

92   Sov. Phys. JETP 55(1), Jan. 1982

Antipov *et al.*   92

shown that if the vortices are excited by a pumping disk of 1.2 cm diameter, no (anticyclonic) perturbations of any amplitude can produce long-lived vortices. It can therefore be assumed that the choice of the 3-cm pumping disk is the optimum: it corresponds to the best generation of such vortices that subsequently live long enough.

In the next measurement run a camera rotating together with the paraboloid, photographed the velocity field in the vortices as well as the white particles floating on the surface of the working liquid. Figure 9 shows examples of single vortices photographed 2–3 sec after stopping the pumping disk. As in the preceding photographs, all the single vortices are anticyclones. This is seen both from the darkening of the vortex region and from Fig. 9c, which was photographed before the pumping disk was stopped. Since the paraboloid rotates counterclockwise and the disk clockwise (see Fig. 2), it is clear from Fig. 9c that the produced vortex is an anticyclone (the particles are rotated in a direction opposite to the vessel rotation). From photographs of this type it is easy to determine independently all the vortex parameters: their size, spatial structure, amplitude, intrinsic angular velocity, and drift velocity. It must be recognized here that since the vortex rotates and drifts simultaneously, the total velocity of a particle on the outer edge of the vortex (farther from the center of the paraboloid) is higher than on the inner edge. A comparison of these velocities makes it possible to determine both the intrinsic-rotation and the drift velocity of the vortex. The drift velocity determined by this method agrees with the preceding measurements.

Typical profiles of the linear velocity of the particle's own rotation in the vortex $v_\rho(\rho)$ and of the angular velocity $\omega_\rho = v_\rho/\rho$ (where ρ is the distance from the center of the vortex) are shown in Fig. 10. The characteristic velocity v_r corresponding to the half-width of the profile $\omega_\rho(\rho)$ can be connected with the vortex amplitude by using the approximate geostrophic-equilibrium condition

$$2v_r\Omega_0\cos\alpha \approx g^*H_i h/a, \qquad (17)$$

which corresponds to relation (6) apart from replacement of g by $g^* = g/\cos\alpha$. From (17) and the measured values of v_r and a it is possible to determine the amplitude h. The data obtained in this manner agree with the results of photometry of the vortices, both with respect to the amplitudes and with respect to the charac-

ter of the profiles and their widths (cf. Figs. 7 and 10). These profiles, as seen from Fig. 10, are also of the soliton type. The regimes under which the photographs in Figs. 9 and 10 were taken correspond to amplitudes $h = 0.5–0.7$. Under these conditions, in accord with the measurements described above and based on the photometry of the vortices (Fig. 7), the diameter of the investigated anticyclones, determined from velocity profiles of the type shown in Fig. 10, turns out at $H_0 = 0.5$ to be ~(4.5–5) cm ≈ $2.5r_R$, i.e., smaller by approximately a factor 2–3 than called for by the theoretical equation (4).

Figure 5, which was already considered in part before, shows a comparison of one and the same vortex at two instants of time, at approximately 10 and 18 sec after stopping the pumping disk. It is seen that the vortex manages to drift during its lifetime a distance not less than 10 of its own diameters. It reveals no tendency to spreading, thereby differing in principle from a linear wave packet. In other words, the considered vortex is a (nonlinear) solitary wave or a soliton.

Another important question is that of the character of the interaction between a vortex drifting in a liquid and the particles it encounters in its path. The fact that all the particles contained in the vortex at a given instant are set in rotation by the vortex is clearly seen in the photographs of Fig. 9. But are the particles also made to drift? To answer this question, experiments were performed, in which test particles were injected (from above, as already mentioned) as well as in front of the vortex. These experiments yielded the following results. First, they showed that the vortex captures and retains the particles that enter in it (from above), both those floating on the surface of the working liquid and those dissolved in its volume. This is illustrated by Figs. 5a and 5b, from which it is seen that the potassium-permanganate droplets drift with the vortex and do not lag it. Second, these experiments have shown that the test particles introduced not in the vortex itself but in front of it are pushed apart by the vortex and flow around it without entering the vortex. This is seen from the motion pictures in Fig. 11, in which the test particles are small paper circles.

The experimental data presented here[2] can be interpreted theoretically as follows. Under the typical conditions of our experiments, particularly under the conditions in which we investigated the interaction between the vortex and liquid particles, the vortex amplitude was of the order of $h \approx 0.5$. In vortices of these amplitude, as shown by the described measurements, the characteristic intrinsic vortex angular velocity v_r is several times larger than the drift velocity V_x. This means that the following condition holds

$$v_r \gg V_x, \qquad (18)$$

which, incidentally, is numerically close to the condition (8) under which the vortex is not broken up by the drift-velocity gradient. This condition however, determines decisively the character of the interaction between the vortex and the liquid particles. In fact if condition (18) is satisfied, then a particle cannot enter or leave the vortex: otherwise its trajectory would cross
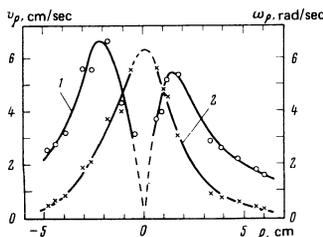
FIG. 10. Spatial profiles of linear velocity $v_\rho(\rho)$ (curve 1) and angular velocity $\omega_\rho(\rho)$ (curve 2) of the vortex's own rotation. The abscissas are the distances ρ from the center of the vortex. It is useful to compare this figure with Fig. 7.
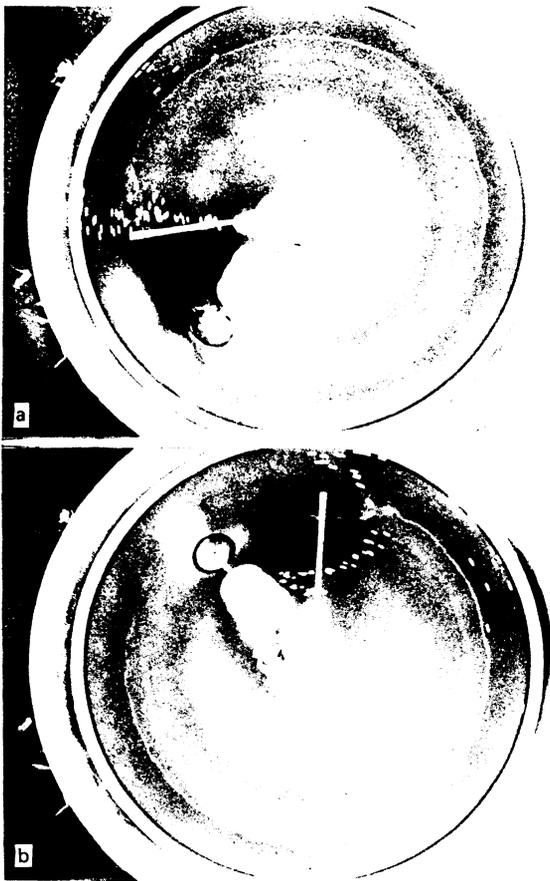
FIG. 11. Interaction of vortex with white particles injected from the top into the region in front of the vortex with the aid of a catapult displaced at an angle 45° in the clockwise direction relative to the direction to the pumping disk (the catapult is seen as a white straight line). The time intervals between the frames equal 1 sec. It is seen that the floating particles flow around the vortex.

a current line in the vortex, which is impossible. This means that the vortex must drift together with "its own" particles and should not capture those particles which it encounters as its drift relative to the liquid. These

FIG. 12. Breakup of vortices of excessively large dimensions into zonal flows.

arguments agree with the experimental data presented in Figs. 5 and 11.

A series of experiments were performed with a liquid of larger depth, with H_0 that was varied between 0.5 and 1.2 cm. The experiments have shown that an increase of H_0 causes a considerable increase of the drift velocity and the transverse dimensions of the vortices, in agreement with the theoretical relations (4), (15), (16), and (16'). As for the vortex lifetime, despite the substantial decrease of the viscosity effect with increasing H_0, the lifetime does not increase (!). The reason for this circumstance (as well as an illustration of the increase of the drift velocity and the vortex dimensions) is seen from Fig. 12: larger vortices break up into zonal flows. Thus, in the case of Fig. 12, the first vortex (which drifts in front) has already broken up, and a similar fate is expected for the second vortex that follows it: only zonal flows remain after 1 sec.

Figures 8a and 8b show examples of the vortex structures already mentioned earlier. From the contrast between the dark and light places on the photographs it is easier to distinguish the anticyclones from the cyclones. Vortices of opposite signs are distinguished also by the different rotation directions and by the separatrices between them. Thus, Fig. 8a shows a pair of cyclone-anticyclone vortices, while Fig. 8b shows a triplet of vortices, two anticyclones and one cyclone between them. It is also seen from Fig. 8 that the particle velocities are clearly lower in the cyclones than in the anticyclones. This confirmed the earlier conclusion that the cyclones are secondary formations, i.e., that there is a fundamental asymmetry in the conditions for the existence of vortices of opposite signs. This asymmetry is observed also in different form: it is possible to choose experimental conditions such that (independently of the direction of the pumping-disk rotation) the same result is obtained: a long-lived anticyclone-cyclone pair is produced (the vortices are located one behind the other), drifting towards a single anticyclone. This asymmetry of the vortices of opposite signs is a weighty qualitative argument favoring the theory of Ref. 2. It offers also evidence that the cyclone-anticyclotron pairs described in the theoretical paper by Larichev and Reznik[3] are not realized under the conditions of our experiments: according to Ref. 3 the vortices of both signs should be "on a par" in these pairs.

To conclude this section, we emphasize the fundamentally important result of the experiments with pure water as a working liquid. It means that increasing the viscosity of the medium by 3–4 times does not eliminate the quantitative discrepancy, noted above, between the theory of Ref. 2 and experiment: the measured sizes and drift velocities of the Rossby solitons turn out to be smaller by a factor 2–3 than the theoretical values, and this discrepancy does not depend on the viscosity of the medium. The cause of this discrepancy calls for further study.

CONCLUSIONS

Let us summarize the main results of the work.

1. In a thin layer of a uniformly rotating liquid, long-lived solitary vortices were produced and negotiated during their lifetime, which is determined by the viscosity of the medium, a path exceeding their diameter by an order of magnitude, without exhibiting a tendency to spread.

2. The long-lived vortices are geostrophically equilibrium anticyclones. There exist no long-lived single cyclones. This means that the observed vortices are in principle nonlinear formations.

3. The vortices drift in a direction opposite to the liquid motion and rotate about their own vertical axis in a direction opposite to the global rotation of the liquid.

The velocities of the drift and of the intrinsic rotation of the vortices correspond in the main to the theoretically expected characteristics of Rossby solitons. The regularities of the variation of the vortex drift velocity with changing system parameters correspond to the properties of Rossby waves (solitons).

5. The dimensions of the observed vortices correspond in the main to the theoretically expected dimensions of the Rossby solitons. Excitation of regions of smaller size does not lead to formation of long-lived vortices. Excitation of a larger zone causes the latter to break up into a system of vortices whose dimensions correspond to those of the Rossby solitons.

6. The totality of the formulated conclusions means that the anticyclonic vortices observed in the present study are solitary Rossby waves (solitons). Rossby solitons were experimentally produced and investigated for the first time ever in the present study (including Ref. 1).

7. Large-amplitude Rossby solitons interact with liquid particles quite uniquely: the particles inside the vortex are made to drift with it, while the "extraneous" particles flow around the vortex.

8. The conditions under which Rossby solitons break up into zonal flows were found.

9. This study is on the whole a confirmation (with a more or less adequate model) of the theory of Ref. 2, which in turn agrees with experiment not only qualitatively but also quantitatively, accurate to not more than within a numerical factor 2–3.

10. Thus, the present paper can be regarded as supporting the soliton model of the Jupiter spot.[2,4,23]

11. Since Rossby waves and solitons are similar to drift waves and drift solitons in a plasma, it can be assumed that in the present study we have successfully simulated drift solitons.

[1] Strictly speaking, to produce a layer of constant depth the shape of the vessel was chosen somewhat different from parabolic: the bottom of the vessel was a surface on which each point was equidistant from the parabolic surface of the liquid.

[2] These data can be of definite interest for oceanology (see Ref. 28 on this subject).

[1] S. V. Antipov, M. V. Nezlin, E. N. Znezhkin, and A. S. Trubnikov, Pis'ma Zh. Eksp. Teor. Fiz. 33, 368 (1981) [JETP Lett. 33, 351 (1981)].

[2] V. I. Petviashvili, ibid. 32, 632 (1980) [32, 619 (1980)].

[3] V. D. Larichev and G. M. Reznik, Dokl. Akad. Nauk SSSR 231, 1077 (1976).

[4] T. Maxworthy and L. G. Redekopp, Icarus 29, 261 (1976); Science, 210, 1350 (1980).

[5] A. S. Monin and M. N. Koshlyakov, in: Nelineĭnye volny (Nonlinear Waves), Nauka, 1979.

[6] A. M. Obukhov, G. S. Golitsyn, and F. V. Dolzhanskiĭ, in: Nekotorye problemy sovremennoĭ fiziki atmosfery (Some Problems in Modern Atmospheric Physics), Nauka, 1981.

[7] L. A. Diky and G. S. Golitsyn, Tellus 20, 314 (1968).

[8] R. A. Madden, Rev. Geophys. Space Phys. 17, 1935 (1979).

[9] E. N. Parker, Asterophys. J. 162, 665 (1970).

[10] A. S. Monin, Usp. Fiz. Nauk 132, 123 (1980) [Sov. Phys. Usp. 23, 594 (1980).

[11] A. Hasegawa, S. G. Maclennan, and Y. Kadama, Phys. Fluids 22, 122 (1979).

[12] V. I. Petviashvili, Fiz. Plazmy 3, 270 (1977) [Sov. J. Plasma Phys. 3, 150 (1977)].

[13] B. B. Kadomtsev, in: Voprosy teorii plazmy (Problems of Plasma Theory), M. A. Leontovich, ed., Vol. 4, Atomizdat, 1964, p. 269.

[14] A. B. Mikhaĭlovskiĭ, Theory of Plasma Instabilities, Plenum, 1976, Chap. 2.

[15] E. Scott, transl. in: Volny v aktivnykh i nelineĭnykh sredakh i prilozheniya k élektronike (Waves in Active and Nonlinear Media and Applications to Electronics), Appendix I, Sov. radio, 1977.

[16] C. Rebbi, Scientific American 240 (2), 92 (1979).

[17] G. W. Platzman, J. Roy. Meteor. Soc. 94, 225 (1968).

[18] S. G. Rossby, J. Marine Res. 2, 38 (1939).

[19] V. M. Kamenkovich and A. S. Monin, Gidrodinamika okeana (Hydrodynamics of the Ocean), Nauka, 1978, Chap. 1.

[20] V. M. Kamenkovich and G. M. Reznik, ibid. Chap. 7.

[21] B. B. Kadomtsev, Kollektivnye yavleniya v plazme (Collective Phenomena in Plasma), Nauka, 1976, Chap. 3. V. I. Karpman, Nonlinear Waves in Dispersive Media, Pergamon Press.

[22] J. Lighthill, Waves in Liquids (Russ. transl.), Mir, 1981.

[23] M. V. Nezlin, Pis'ma Zh. Eksp. Teor. Fiz. 34, 83 (1981) [JETP Lett. 34, 77 (1981)].

[24] N. A. Philips, Tellus 17, 295 (1965).

[25] H. P. Greenspan, Theory of Rotating Fluids, Cambridge U. P., (1968).

[26] F. V. Dolzhanskiĭ, M. V. Kurganskiĭ, and Yu. L. Chernous'ko, Izv. AN SSSR, fiz. atmosf. i okeana 15, 597 (1979).

[27] Yu. L. Chernous'ko, ibid. p. 1084.

[28] M. N. Koshlyakov, Yu. M. Grachev, and V. Enikeev, Dokl. Akad. Nauk SSSR 252, 573 (1980).

Translated by J. G. Adashko